IEEE Access
Multidisciplinary | Rapid Review | Open Access Journal

Received January 26, 2021, accepted February 10, 2021, date of publication February 19, 2021, date of current version March 9, 2021.

Digital Object Identifier 10.1109/ACCESS.2021.3060398

Miniature Convoluted FSS for Gain Enhancement of a Multiband Antenna

GARTH D. CATTON, (Member, IEEE), HUGO G. ESPINOSA, (Senior Member, IEEE), ALIYA A. DEWANI, (Member, IEEE), AND STEVEN G. O'KEEFE
School of Engineering and Built Environment, Griffith University, Nathan, QLD 4111, Australia

Corresponding author: Garth D. Catton (g.catton@griffith.edu.au)

This work was supported in part by Griffith University through the Research Training Program and in part by the Australian Commonwealth Government.

ABSTRACT Convoluted elements on a frequency selective surface (FSS) allow for low frequency elements to be contained in physically smaller unit cells. Smaller unit cells give the FSS greater angular stability, especially where a curved FSS is required, and so unwanted grating effects are avoided. A convoluted element FSS with a frequency rejection band centred at 2 GHz and unit cell area of 15 mm by 15 mm ($0.10\,\lambda \times 0.10\,\lambda$) has been developed. To test its usefulness, the full structure FSS is used as a parabolic reflector in a dual band FSS reflector antenna operating at 1 GHz and 2 GHz. Simulated and measured results are close at both bands. The reflector antenna has high gain at 2 GHz of 12.7 dBi (simulated) and 11.7 dBi (measured). To observe the angular stability of the FSS and therefore its effectiveness as a reflector, it was compared with a copper test reflector at both bands. Simulation of the reflector antenna with test reflector produced a 2 GHz gain of 13.3 dBi which is very close to that with the FSS reflector. The simulated 2 GHz gain plot of the reflector antenna with FSS reflector is very similar to that with the test reflector indicating that the FSS has good angular stability. The gain at 1 GHz is also high with 9.3 dBi (simulated) and 8.7 dBi (measured). Simulation of the reflector antenna with no FSS and only a rear test reflector produced a 1 GHz gain of 10 dBi which is very close to that with the FSS reflector in place indicating that the FSS causes no significant attenuation at that frequency. The convoluted element FSS would be useful as a curved reflector in the creation of high gain, multiband, conformal antennas.

INDEX TERMS Angular stability, convoluted element, dual band, flexible, frequency selective surface (FSS), miniaturisation, reflector antenna.

I. INTRODUCTION

With the roll out of 5G communication infrastructure there is a need for small, conformal, high gain, antennas and often there is a requirement for those antennas to be multiband. Small multiband antennas can be realised using frequency selective surfaces (FSS). As its name implies, an FSS behaves differently depending on the frequency of an incident electromagnetic (EM) wave. FSS have been the subject of much investigation for applications such as microwave and optical filters for more than 50 years [1]–[3]. A band stop FSS consists of a periodic array of conductive elements on a dielectric substrate. It reflects EM waves at one frequency band while EM waves at other bands pass through with minimal attenuation [4]. This characteristic makes the FSS particularly useful when it is used as a frequency dependent reflector (FDR) in a reflector antenna system. The use of an FSS as an FDR allows, for example, feed antennas in separate locations to use a single main reflector thus decreasing size and cost of the antenna and providing the convenience of not needing to realign the reflector dish for each different frequency band. A tri band FSS reflector system was used on the Cassini space mission. Cassini's antenna system employs an initial FSS to reflect X band while passing through S and Ku bands and then a secondary FSS that reflects Ka band and allows S, X and Ku bands to pass through [5]. FSS have also been used more recently as reflectors to enhance antenna gain [6]–[8].

Each periodic element of an FSS are contained in a unit cell and these cells need to display the same frequency response regardless of the angle of incidence or polarisation of an incident EM wave for an FSS to be considered to have frequency response stability. Without this stability an FSS is

The associate editor coordinating the review of this manuscript and approving it for publication was Davide Ramaccia.

of limited practical use. Frequency response stability of an FSS is related to the size of its unit cells with respect to a wavelength [9] and the size of each unit cell is determined by the size of its elements. The length of a conventional FSS dipole element is generally in the order of half a wavelength [4], [10] so at the S band and longer, FSS using these conventional elements are electrically quite large. When FSS at these longer wavelengths are to be used in applications where space is limited, their unit cell size must somehow be reduced.

Smaller unit cells also provide greater angular stability. When ray traces are incident on an FSS unit cell at oblique angles they arrive at different times creating a phase difference between them. Conventional elements at the S band and longer are quite large making this phase difference greater and so the FSS has angular instability. This problem is further compounded if an FSS is curved as the phase difference of the ray traces incident on each unit cell is further increased. When the unit cells of an FSS are miniaturised this phase difference is greatly reduced.

One method of reducing unit cell size, thereby miniaturising the FSS and still maintaining frequency response stability, is by using ultra-thin dielectric substrates [11]–[13] to separate multiple layer FSS. The high capacitance created by the ultra-thin substrate causes a lower resonant frequency due to (1). Where f_r is the resonant frequency, L is the total inductance and C is the total capacitance in an FSS unit cell.

$$f_r = {}^{1}\!/_{2\pi\sqrt{LC}} \tag{1}$$

Metamaterials are also used to miniaturise FSS elements. In [14] a design method based upon the theory of metamaterials uses an equivalent circuit model with lumped elements to design a miniaturised FSS. Metamaterials are used again in [15] where a resistive sheet and a planar array of resonating magnetic inclusions are placed in close proximity to design miniaturised microwave absorbers.

Another technique [16] to miniaturise FSS unit cells is by convoluting the conductive trace elements within them. Convoluted elements have much longer path lengths than the more conventional dipole, ring or square elements, and in the same unit cell area. The longer traces produce more inductance per unit cell and a lower resonant frequency due to (1). The convoluted elements make it possible to retain frequency response stability with an FSS unit cell that is smaller in size than conventional element FSS. Smaller unit cells help to isolate the fundamental frequency of the FSS from grating lobes [16] which is especially useful when there is a requirement for the FSS to be curved.

A convoluted element FSS was chosen for this experiment because an FSS with a stop band centred at 2 GHz has been developed by screen printing suitably convoluted silver ink trace elements onto a thin flexible substrate [17]. The flexibility of its substrate and its small unit cell size makes it suitable to curve into a parabolic reflector for a reflector antenna system.

To test the angular stability of this FSS and its suitability in such a system, a dual band reflector antenna system using this FSS as an FDR has been designed [18] and fabricated. The reflector antenna consists of two parabolic reflectors to enhance the gain of a dual band trapped dipole. The reflector closest to the trapped dipole is the convoluted FSS with a stop band centred at 2 GHz and so reflects EM waves at that frequency. The rear reflector is made from copper sheet and reflects EM waves at all frequencies.

A trapped dipole was chosen as the feed for the reflector antenna because it is simple to fabricate and provides the required dual band functionality with good illumination over both reflectors. There was also a desire to make the reflector antenna light and compact and it was considered that a horn or waveguide feed would make it heavy and bulky. The trapped dipole operates as a half wave dipole at each of its bands (1 GHz and 2 GHz). The addition of the FSS and rear reflectors focus the EM waves at each band and so a much greater gain than that of a half wave dipole on its own (2.15 dBi [19]) is obtained. While the design of this antenna makes it quite compact, the aim of this paper is not to design a better, smaller dual band trapped dipole. It is to demonstrate the usefulness of the convoluted element FSS as a dual band reflector.

II. ANTENNA DESIGN

A. TRAPPED DIPOLE DESIGN

The trapped dipole consists of two sets of two cylindrical copper rod sections, one set for each of its two elements. The copper rod is 2 mm in diameter. Each set of the two rod sections of each dipole element are connected by a resonant or trap circuit consisting of a capacitor and inductor in parallel (L = 3.3 nH and C = 1.9 pF). The inductor and capacitor (LC) are connected in parallel between each of the two rod sections of the dipole elements creating an electrical connection between them as shown in Fig. 1(a). The values of the inductor and capacitor were chosen using (1) so that each LC parallel circuit resonates at 2 GHz and so present an electrical open circuit at that frequency.

The trapped dipole was modeled using CST Microwave Studio (MWS) EM simulation software and to simulate its trap circuit an LC, parallel circuit, lumped element was connected across each of the 5 mm gaps between the centre faces of the inner and outer elements on each side of the trapped dipole. The lumped element's capacitor value was set to C = 1.9 pF and the inductor value was set to L = 3.3 nH. Lumped elements can present problems in CST MWS when their wire radius is greater than the surrounding mesh cell lines. This problem was averted by setting the radius of the lumped element to zero in the ''Lumped Network Element'' settings.

The 2 GHz resonant trap circuit creates an open circuit and therefore two electrically shortened elements at that frequency. The distance from the dipole feed to the trap is approximately one quarter wavelength at 2 GHz so when the trap is at resonance, a halfwave dipole is effectively created

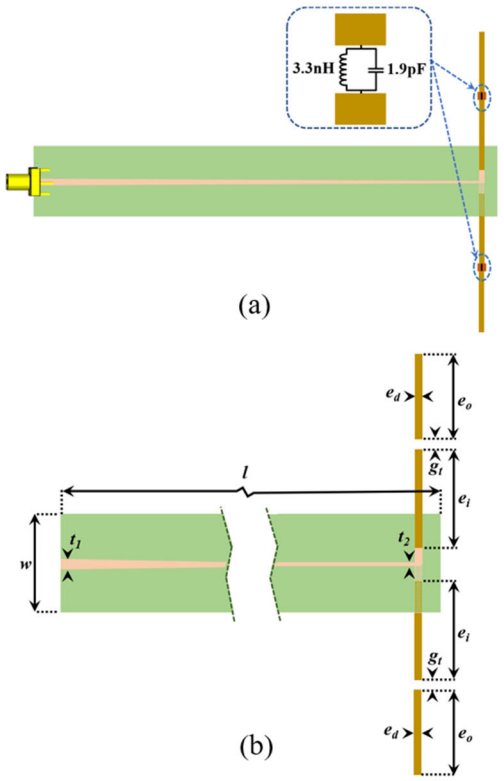

FIGURE 1. (a) Front view of the trapped dipole with MSL feed showing the LC trap circuit, components and values. (b) Truncated front view of the trapped dipole and MSL feed with component dimensions.

TABLE 1. Trapped dipole dimensions.

Parameters	Description	Dimensions
e_i	Inner element length	30 mm
e_o	Outer element length	26 mm
e_d	Element diameter	2 mm
g_t	Trap gap width	5 mm
t_1	MSL topside trace width SMA end	1.6 mm
t_2	MSL topside and underside trace width dipole end	0.8 mm
t_3	MSL underside balun trace width SMA end	30 mm
t_4	MSL underside balun trace width (120 mm from SMA)	1 mm
w	MSL PCB width	30 mm
l	MSL PCB length	200 mm

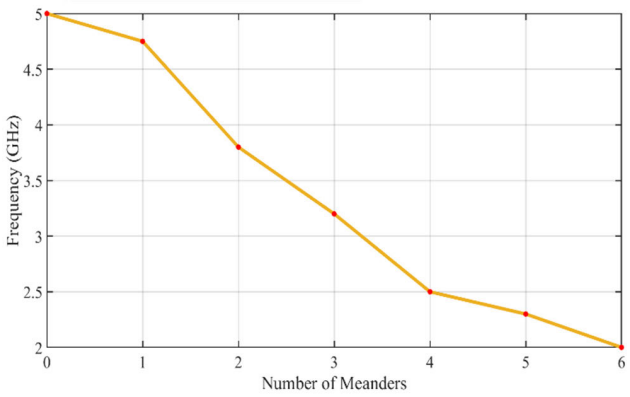

FIGURE 2. Number of meanders of the convoluted FSS and resonant frequency produced.

at that frequency. The trap appears as an electrical short circuit to signals at 1 GHz. The distance from the dipole feed, through the trap, to the end of the outer section of the dipole element is approximately one quarter wavelength at 1 GHz and so a halfwave dipole is created at that frequency. The trapped dipole is therefore dual band, resonating at 1 GHz and 2 GHz.

The dimensions of the various components of the trapped dipole are shown in Fig. 1(b) and Table 1. The trapped dipole is fed via an SMA connected to an impedance matching double-sided-parallel (DSP) microstrip line (MSL). Each of the two elements of the dipole are soldered on either side of the DSP MSL printed circuit board (PCB).

B. FSS DESIGN

To obtain the desired 2 GHz stop band properties in a miniaturised FSS, the elements of a conventional square loop 5 GHz stop band FSS as shown in Fig. 3(a) were convoluted. This produced the much lower resonant frequency of 2 GHz and in the same unit cell area as the original square loop FSS. After extensive simulations in CST MWS, meandered peaks were found to provide the most successful method of maximising element length inside the same unit cell area as the original square loop thereby reducing the stop band to 2 GHz. As part of the many CST MWS simulations of different convolutions of the square loop FSS the effects of trace length, width and separation, and number of meanders on the frequency response of the FSS were all considered.

The most successful design consisted of convoluting half of each side of the square loop FSS into a set of meandered peaks followed by the same number of inverted meandered peaks for the other half side. The meanders were increased from zero, in the case of the square loop FSS, by one meander for each simulation in CST MWS, and the resonant frequency of the new convoluted FSS recorded. As the convoluted FSS design needed to be screen printed onto a polyethylene terephthalate (PET) substrate, the maximum number of meanders was limited to six because of screen printing tolerances. The recorded resonant frequency with respect to number of meanders is shown in Fig. 2.

The final design with a set of three meandered peaks followed by an inverted set of three meandered peaks is shown in Fig. 3(b). Each unit cell of the FSS consists of four convoluted elements joined in a loop as shown in Fig. 3(b) and are printed onto a PET sheet. The dimensions of the FSS unit cell elements are shown in Table 2. A flat sheet of full structure FSS as shown in Fig. 3(c) was used to create the FSS parabolic reflector. When simulated in CST MWS the FSS has a stop band centred at 2 GHz and so makes a good reflector at that frequency..

TABLE 2. FSS unit cell element dimensions.

Parameters	Description	Dimensions
L_0	Square loop element length	14.3 mm
L_1	Convoluted element length	12 mm
L_2	Outer peak to outer peak	18 mm
L_3	Outer peak to inner peak	12 mm
L_4	Peak length	3 mm
P	Unit cell side (square loop & convoluted element FSS)	16 mm
d_1	Peak thickness	1.125 mm
d_2	Trace width (square loop & convoluted element FSS)	0.38 mm
d_3	Peak to peak	2 mm
θ	Peak angle	20°

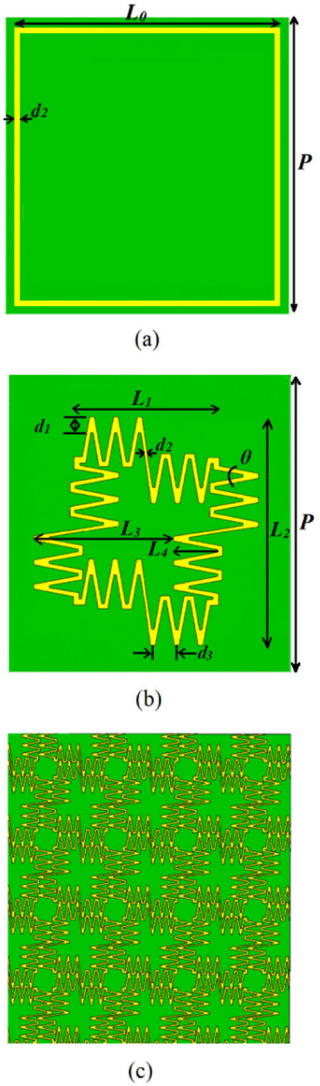

FIGURE 3. (a) Original square loop FSS cell. (b) Convoluted FSS unit cell element dimensions. (c) Full structure FSS.

Plots of the transmission and reflection coefficients of the stand-alone FSS are shown in Fig. 4. At 2 GHz the stand-alone FSS has a null of −41.71 dB for S_{21} while its S_{11} reading is −0.09 dB. At 1 GHz the stand-alone FSS has an S_{21} reading of −5.86 dB while its S_{11} reading is −15.90 dB.

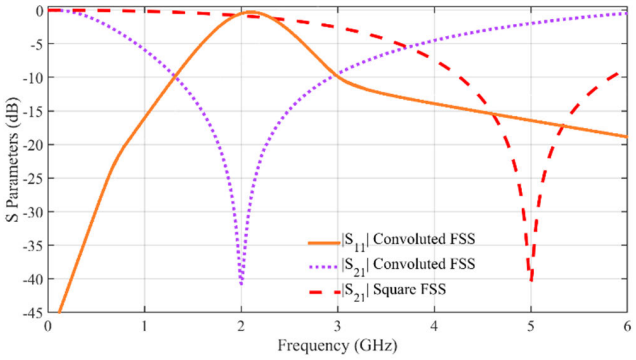

FIGURE 4. Simulated transmission and reflection coefficients of the stand-alone convoluted FSS and transmission coefficient of the stand-alone square FSS.

S_{21} of the square loop FSS is also shown in Fig. 4 and is −40.48 dB at 5 GHz.

C. MSL FEED DESIGN

In order to position the trapped dipole at the correct distance from the two reflectors it's fed by a 200 mm long, DSP MSL etched onto a PCB. The DSP MSL was chosen as it allows for easy soldering of the copper trapped dipole elements. The PCB has an FR4 ($\varepsilon_r = 4.3$) substrate height of 0.8 mm and copper trace height of 0.018 mm (0.5 ounce). All parts of the MSL feed were modelled in CST MWS. As the antenna prototype needed to be connected to a vector network analyser (VNA) for measurement, an SMA connector was also modelled in CST MWS, and fed by a 50 Ω discrete port to simulate the impedance of the VNA.

To facilitate maximum power transfer into the dipole, the MSL is designed such that its impedance is the same as the trapped dipole's 75 Ω impedance (average impedance at 1 GHz and 2 GHz from CST MWS simulation) at one end and the VNA's 50 Ω impedance at the other end. For optimum impedance matching, the widths of the copper trace at each end of the MSL feed were varied using the parameter sweep function in CST MWS. The widths that provided the lowest S_{11} at each band of the reflector antenna were then chosen for fabrication of the prototype. The final design of the topside of MSL PCB has copper trace width of 1.6 mm at the SMA connector end tapering to 0.8 mm at the trapped dipole end and is shown in Fig. 5(a).

In order to allow maximum power transfer from the unbalanced VNA to the balanced trapped dipole, a tapered balun [20] was also modelled, simulated and optimised in CST MWS. The balun which is printed on the reverse side of the MSL PCB has a copper trace width of 30 mm at the SMA connector end, tapering to a 1 mm width over a length of 120 mm and then tapering for a further 80 mm until it reaches the trapped dipole end where it is 0.8 mm wide. The topside and underside traces then turn 90° outwards to create the pads on which the trapped dipole is soldered. The dimensions of the MSL PCB and its topside and underside traces are shown in Fig. 1(b), Fig. 5(a), Fig. 5(b) and Table 1.

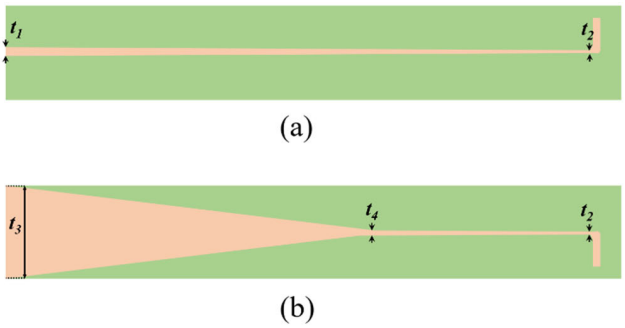

FIGURE 5. (a) Topside of the MSL PCB showing impedance matching tapered MSL trace. (b) Underside of the MSL feed showing tapered balun trace.

D. FSS AND COPPER PARABOLIC REFLECTORS DESIGN

The FSS reflector and copper sheet rear reflector were both modelled in CST MWS as parabolic reflectors. A full structure FSS, as shown in Fig. 3(c), was used to make the FSS reflector. An FSS sheet consisting of 15 unit cells ×15 unit cells (225 mm × 225 mm × 0.048 mm) was modelled with a parabolic curvature and a focal point equal to one quarter wavelength at 2 GHz (37.5 mm). When curved the FSS reflector is 225 mm long with a 187 mm diameter across the curvature, from edge to edge. A copper sheet (225 mm × 225 mm × 0.5 mm) was modelled with a wider parabolic curvature to create the rear reflector. The rear reflector has a focal point equal to one quarter wavelength at 1 GHz (75 mm). When curved, the rear reflector is 225 mm long with a 200 mm diameter across the curvature, from edge to edge. The rear reflector is the largest part of the complete reflector antenna when viewed from the front making it comparable in size to state of the art compact antennas. For example, Australi's national broadband network (NBN) uses a fixed wireless antenna for its customers in isolated areas. Its design is compact and unobtrusive because it must be attached to the exterior of custome's homes but at 450 mm × 450 mm [21] it is still twice as large as this reflector antenna.

The FSS and rear reflectors were initially positioned 37.5 mm apart, with their inside curves facing the +Z direction, and axes of symmetry parallel to the Z axis. The trapped dipole was positioned 37.5 mm above the FSS reflector and along the Y axis so that it was in the focal point of each parabola. This position of the trapped dipole relative to the two reflectors, increases gain in the +Z direction at 1 GHz and 2 GHz.

Using CST MWS simulations, it was found that the antenna's gains at both bands were optimised when the distance from the trapped dipole of the FSS and rear reflector were 39.1 mm and 76.8 mm, respectively. A perspective view of the reflector antenna as it was modelled in CST MWS is shown in Fig. 6(a). Each reflector's distance from the trapped dipole and their dimensions are shown in Fig. 6(b). Reflector dimension values are listed in Table 3.

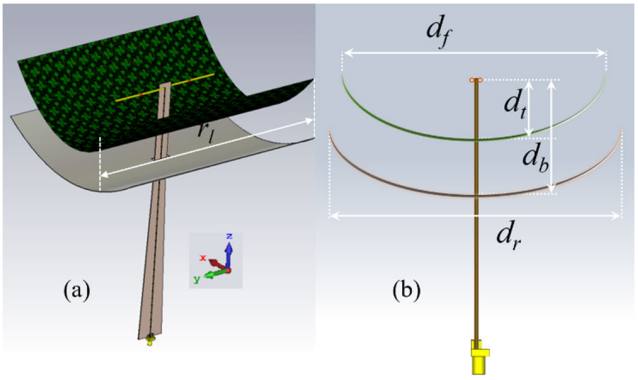

FIGURE 6. (a) Perspective view of the complete reflector antenna with trapped dipole, FSS, rear reflector, MSL feed and SMA connector as modelled for simulation in CST MWS. (b) Side view of the reflector antenna showing dimensions of the FSS and rear reflectors and their distances from the trapped dipole.

TABLE 3. Reflector dimensions.

Parameters	Description	Dimensions
d_f	Diameter FSS reflector	187 mm
d_r	Diameter rear reflector	200 mm
d_t	Trapped dipole to FSS	38.1 mm
d_b	Trapped dipole to rear reflector	76.8 mm
r_l	FSS and rear reflector length	225 mm

III. ANTENNA FABRICATION

A. MSL FEED FABRICATION

The MSL was etched onto a 200 mm × 30 mm PCB with a 0.8 mm thick FR4 ($\varepsilon_r = 4.3$) substrate and 0.018 mm (0.5 ounce) copper trace. An SMA connector was soldered onto the 50 Ω end of the MSL. To test the impedance matching effectiveness of the MSL, a 75 Ω resistor was soldered between the two ends of the MSL at the trapped dipole end to model the impedance of the trapped dipole. The VNA was then connected to the SMA connector and S_{11} was measured. The measurement and CST MWS simulation of S_{11} for the MSL impedance matching test are shown in Fig. 7. At 1 GHz, S_{11} is −25.6 dB and −23.5 dB for the simulated and measured results, respectively. At 2 GHz, S_{11} is −19.9 dB and −18.4 dB for the simulated and measured results, respectively. The low S_{11} values at both bands indicate low reflections and that the MSL provides good impedance matching between the VNA (50 Ω) and the trapped dipole (75 Ω). The 75 Ω resistor was then de-soldered from the MSL and the trapped dipole's element inner sections were soldered in its place.

B. TRAPPED DIPOLE FABRICATION

To fabricate the trapped dipole, two sets of capacitors and inductors were soldered in parallel and onto each end of two sets of two copper cylindrical rod sections that are each 2 mm in diameter. Surface mount technology (SMT) components were chosen because their small size allows them

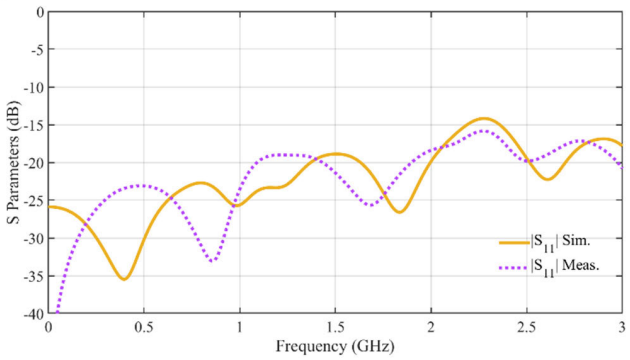

FIGURE 7. Simulated and measured S_{11} results of the MSL feed when the trapped dipole was replaced with a 75 Ω resistor to test the impedance matching effectiveness of the MSL feed.

FIGURE 8. The capacitor and inductor of the 2 GHz trap are soldered together in parallel and to the inner and outer sections of the elements.

to be soldered to the narrow ends of the copper rod sections. The inductors and capacitors chosen are standard SMT size, 0805 (2.0 mm × 1.3 mm), and have values of C = 1.9 pF and L = 3.3 nH, respectively. The components of the trap circuit as they are soldered onto the inner and outer ends of the dipole element's copper rod sections are shown in Fig. 8.

Before the LC components of the trap were soldered in between the two sections of the dipole elements, the inner section lengths were tuned for 2 GHz. To do this the inner sections of the dipole elements were cut a little longer than the lengths designed in CST MWS and soldered onto the trapped dipole end of the MSL PCB. The S_{11} measurement at 2 GHz on the VNA was then optimised by trimming the inner section ends with wire cutters. After the inner sections of each dipole element were calibrated for 2 GHz, the trap components were then soldered onto the outer ends of the inner element sections and the inner ends of the outer element sections. The ends of the outer element sections, which had also been cut a little longer, were then trimmed for optimal S_{11} results at 1 GHz. To solder the trap components in place, low melting point solder was used so that the dipole element inner sections did not become de-soldered from the MSL PCB. After the trapped dipole was tuned at both frequencies, the solder connections of the SMT components were reinforced with heat shrink insulation as shown in the fabricated reflector antenna prototype in Fig. 9. After tuning for each band of operation, the optimised trimmed lengths of the inner

FIGURE 9. The complete fabricated reflector antenna prototype with the trapped dipole soldered to the MSL feed, FSS and rear reflectors, SMA connector and polystyrene mounts.

and outer copper rod sections of each element of the trapped dipole were 30 mm and 26 mm, respectively.

C. FSS AND REAR REFLECTOR FABRICATION

A hot wire and 5 mm thick acrylic plastic cutting guides that had been laser cut to the required parabolic curves, were used to shape three pairs of 50 mm polystyrene mounts for the FSS and rear reflectors. Polystyrene was used for mounting the reflector antenna because it has a dielectric constant close to air and is easily and accurately cut with a hot wire. The FSS and copper sheets were then curved and glued to the mounts using polyvinyl acetate (PVA) glue to form the FSS and rear reflectors. Small rectangular holes were cut into both the FSS and rear reflectors to allow the MSL feed to pass through them without making any electrical connection. The mounts were glued to a polystyrene base to strengthen and stabilise the reflector antenna prototype. Access to the reflector antenna's SMA connector feed is via a 20 mm diameter hole in the base. Polystyrene was also used to hold the MSL PCB and other parts of the reflector antenna in place. The complete reflector antenna prototype including its trapped dipole, FSS and rear reflectors with their polystyrene mounts, and MSL feed with SMA connector, is shown in Fig. 9.

IV. RESULTS

A. MEASUREMENT SET UP

The reflector antenna was tested in an anechoic chamber using a VNA (Anritsu Shockline, model number MS46122B, 1 MHz – 43.5 GHz), two identical gain standard pyramidal horn antennas and antenna mounting apparatus. The reflector antenna gain was measured using the gain standard antenna replacement technique. This technique requires that the distance between the antenna under test (AUT) and the test antenna places them in each other's far field at the frequencies of operation. This is also important as the AUT utilizes an FSS and it's the far field frequency response

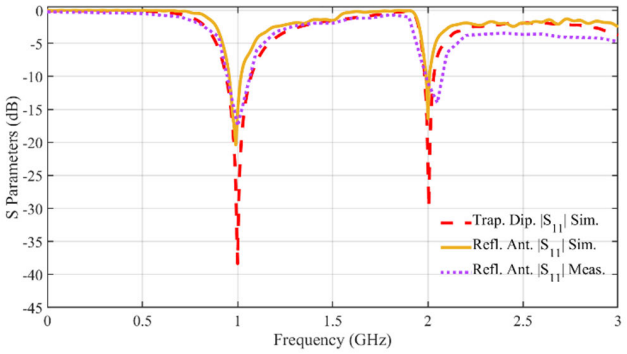

FIGURE 10. Simulated S_{11} for the stand-alone trapped dipole and simulated and measured S_{11} for the reflector antenna.

characteristics of the FSS that are of interest for these measurements. The reflector antenna was rotated in azimuth and elevation and S_{21} was measured using the VNA at each degree increment.

B. FREQUENCY RESPONSE OF THE DUAL BAND REFLECTOR ANTENNA

The reflector antenna's S_{11} parameters as simulated in CST MWS and measurements taken from the prototype using the VNA are shown in Fig. 10. At 1 GHz there is a null of −20.3 dB for the simulation and −17.5 dB for the measurement. At 2 GHz there is a null of −16.5 dB for the simulation. There is a null of −14 dB measured at 2.1 GHz while the S_{11} measurement at 2 GHz was −11 dB.

The measured S_{11} results of the complete reflector antenna are very close to the simulated results at both bands. The nulls of the simulated and measured S_{11} results of the complete reflector antenna are also very close in frequency to the nulls of the stand-alone trapped dipole which are −38.36 dB at 1 GHz and −29.87 dB at 2 GHz as shown in Fig. 10.

C. GAIN OF THE DUAL BAND REFLECTOR ANTENNA

The simulated and measured co and cross polarised gains of the reflector antenna in the E plane at 1 GHz are shown in Fig. 11. The maximum gains in the E plane at 1 GHz for co polarised antennas are 9.3 dBi and 8.6 dBi for the CST MWS simulation and VNA measurements, respectively. The maximum gains in the E plane at 1 GHz for cross polarised antennas are −14.2 dBi and −5.5 dBi for the CST MWS simulation and VNA measurements, respectively. To see how much the FSS attenuates the signal at 1 GHz the FSS was removed and the reflector antenna was then simulated in CST MWS with only the rear copper test reflector. With the FSS reflector removed, simulation of the reflector antenna produced a maximum gain in the E plane at 1 GHz of 10 dBi and is shown in Fig. 11 (1 GHz Test Refl. Sim.). The maximum gain of the stand-alone trapped dipole in the E plane at 1 GHz is 1.87 dBi and is shown in Fig. 11.

The simulated and measured co and cross polarised gains of the reflector antenna in the E plane at 2 GHz are shown in Fig. 12. The maximum gains in the E plane at 2 GHz

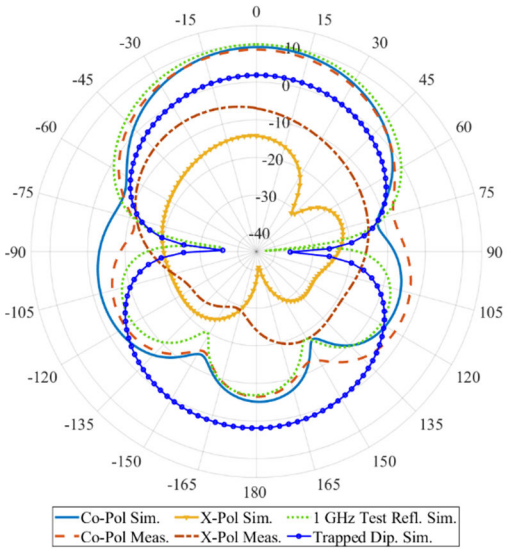

FIGURE 11. Plots of the simulated and measured gain (dBi) for co and cross polarisation of the reflector antenna with FSS and test reflectors and the stand-alone trapped dipole in the E Plane at 1 GHz.

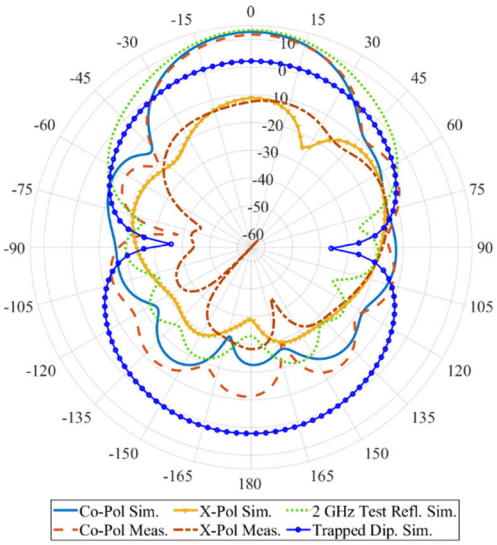

FIGURE 12. Plots of the simulated and measured gain (dBi) for co and cross polarisation of the reflector antenna with FSS and test reflectors and the stand-alone trapped dipole in the E Plane at 2 GHz.

for co polarised antennas are 12.7 dBi and 11.7 dBi for the CST MWS simulation and VNA measurements, respectively. The maximum gains in the E plane at 2 GHz for cross polarised antennas are −11.1 dBi and −11.6 dBi for the CST MWS simulation and VNA measurements, respectively.

To test how well the FSS performs as a reflector at 2 GHz it was replaced in the CST MWS model by a copper test reflector with the same dimensions and parabolic curvature as the FSS reflector. With the copper test reflector in the exact position as the FSS reflector, simulation of the reflector antenna produced a maximum gain in the E plane at

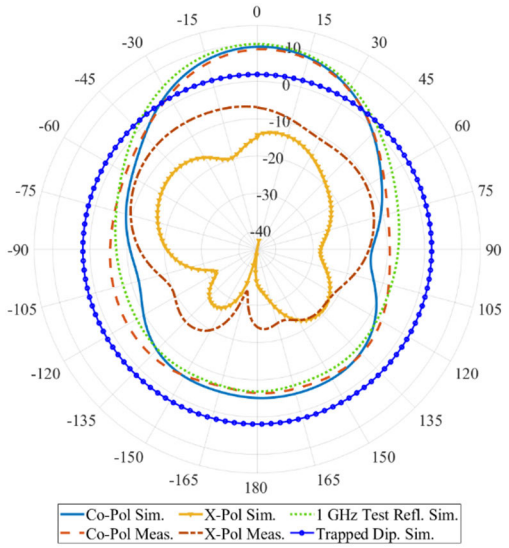

FIGURE 13. Plots of the simulated and measured gain (dBi) for co and cross polarisation of the reflector antenna with FSS and test reflectors and the stand-alone trapped dipole in the H Plane at 1 GHz.

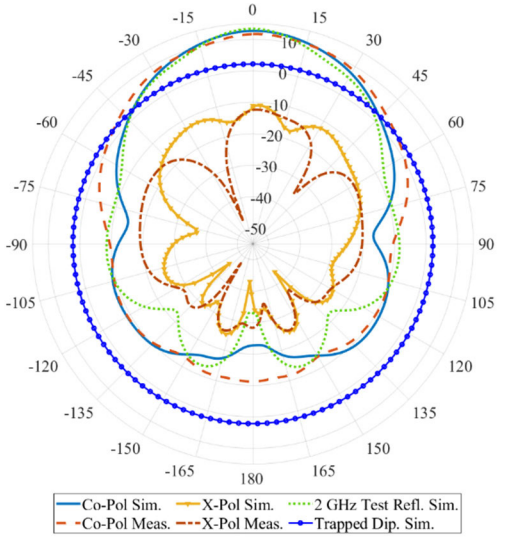

FIGURE 14. Plots of the simulated and measured gain (dBi) for co and cross polarisation of the reflector antenna with FSS and test reflectors and the stand-alone trapped dipole in the H Plane at 2 GHz.

2 GHz of 13.3 dBi and is shown in Fig. 12 (2 GHz Test Refl. Sim.). The maximum gain of the stand-alone trapped dipole in the E plane at 2 GHz is 2.15 dBi and is shown in Fig. 12.

The simulated and measured co and cross polarised gains of the reflector antenna in the H plane at 1 GHz are shown in Fig. 13. The maximum gains in the H plane at 1 GHz for co polarised antennas are 9.3 dBi and 8.7 dBi for the CST MWS simulation and VNA measurements, respectively. The maximum gains in the H plane at 1 GHz for cross polarised antennas are −13.4 dBi and −5.9 dBi for the CST MWS simulation and VNA measurements, respectively.

With the FSS reflector removed, simulation of the reflector antenna produced a maximum gain in the H plane at 1 GHz of 10 dBi and is shown in Fig. 13 (1 GHz Test Refl. Sim.). The maximum gain of the stand-alone trapped dipole in the H plane at 1 GHz is 1.87 dBi and is shown in Fig. 13.

The simulated and measured co and cross polarised gains of the reflector antenna in the H plane at 2 GHz are shown in Fig. 14. The maximum gains in the H plane at 2 GHz for co polarised antennas are 12.7 dBi and 11.7 dBi for the CST MWS simulation and VNA measurements, respectively. The maximum gains in the H plane at 2 GHz for cross polarised antennas are −10.9 dBi and −12.4 dBi for the CST MWS simulation and VNA measurements, respectively.

With the FSS reflector replaced by the copper test reflector, simulation of the reflector antenna produced a maximum gain in the H plane at 2 GHz of 13.3 dBi and is shown in Fig. 14 (2 GHz Test Refl. Sim.). The maximum gain of the stand-alone trapped dipole in the H plane at 2 GHz is 2.15 dBi and is shown in Fig. 14.

The 3D gain plots of the complete reflector antenna at 1 GHz and 2 GHz are shown in Fig. 15(a) and Fig. 15(b),

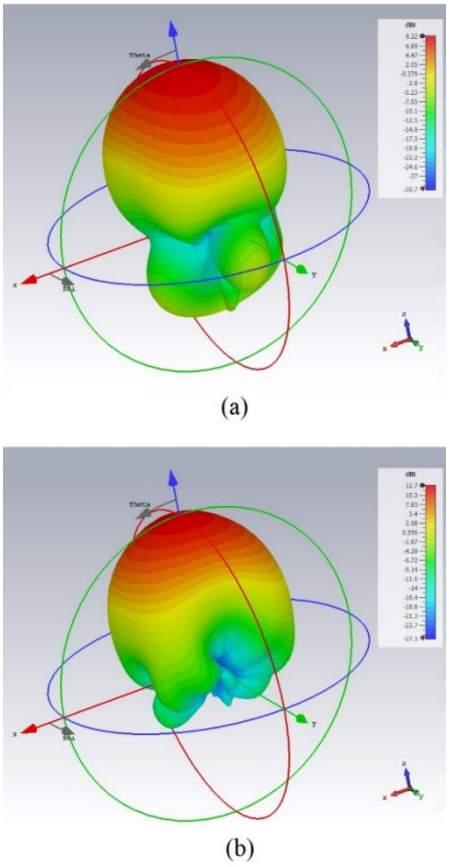

FIGURE 15. Simulated 3D gain plot at (a) 1 GHz and (b) 2 GHz of the complete reflector antenna.

respectively. The gain results indicate that the convoluted element FSS makes a very effective reflector for gain enhancement at its 2 GHz stop band. The FSS requires angular

stability from 0° up to 75° where ray traces are reflected from the reflector's edge. The 2 GHz gain plot using the FSS reflector has a very good match to the test reflector in the E plane out to around 30°, and in the H plane it is an excellent match out to around 70°. This similarity between gain plots of the reflector antenna with FSS reflector and that with an almost perfect reflecting surface, indicates that the FSS has good angular stability.

The 2 GHz gain in both planes using the test reflector is 13.3 dBi and is only a little more than the gain using the FSS reflector which has 12.7 dBi for the simulation and 11.7 dBi for the measured prototype. The 2 GHz gain of the reflector antenna using the FSS reflector is 10.55 dBi (simulated) and 9.55 dBi (measured) greater than that of the stand-alone trapped dipole.

The gain at 1 GHz is also quite good indicating that EM waves at that frequency are passing through the FSS with no significant attenuation. The gain at 1 GHz is 9.3 dBi for the simulation and 8.7 dBi for the prototype measurements which are 7.43 dBi and 6.83 dBi greater than that of the stand-alone dipole.

V. CONCLUSION

The convoluted elements of the FSS allow for frequency response stability using a miniaturised unit cell area at a low stop band of only 2 GHz. A particular innovation of this design is that it allows for the reflector to be curved over a radius that is smaller than a wavelength. The frequency response, angular stability, flexibility and compact size of the 2 GHz stop band convoluted element FSS makes it very suitable for many S band applications where space is limited and a curved FSS is required.

The FSS would be very effective as a compact reflector for multiband directional antenna designs that might be used in applications such as fixed wireless broadband for wireless internet service providers (WISP), or similar. The ease of manufacture, low cost, and ease in forming the thin sheets into different shaped focal structures would allow economic mass manufacture of higher performance antennas for consumer application.

REFERENCES

[1] J. L. Matson and F. A. O'Nians, "Antenna feed system simultaneously operable at two frequencies utilizing polarization independent frequency selective intermediate reflector," U.S. Patent 3 231 892, Jan. 25, 1966.
[2] C.-C. Chen, "Scattering by a two-dimensional periodic array of conducting plates," *IEEE Trans. Antennas Propag.*, vol. AP-18, no. 5, pp. 660–665, Sep. 1970.
[3] B. Munk, R. Kouyoumjian, and L. Peters, "Reflection properties of periodic surfaces of loaded dipoles," *IEEE Trans. Antennas Propag.*, vol. AP-19, no. 5, pp. 612–617, Sep. 1971.
[4] B. A. Munk, *Frequency Selective Surfaces: Theory and Design*. New York, NY, USA: Wiley, 2000.
[5] J. Huang and S. W. Lee, "Tri-band frequency selective surface with circular ring elements," in *Antennas Propag. Soc. Symp. Dig.*, Jun. 1991, pp. 204–207.
[6] A. Chatterjee and S. K. Parui, "Performance enhancement of a dual-band monopole antenna by using a frequency-selective surface-based corner reflector," *IEEE Trans. Antennas Propag.*, vol. 64, no. 6, pp. 2165–2171, Jun. 2016.
[7] S. Mohamad, R. Cahill, and V. Fusco, "Performance of Archimedean spiral antenna backed by FSS reflector," *Electron. Lett.*, vol. 51, no. 1, pp. 14–16, Jan. 2015.
[8] K. Ding, C. Gao, T. Yu, and D. Qu, "Wideband CP slot antenna with backed FSS reflector," *IET Microw., Antennas Propag.*, vol. 11, no. 7, pp. 1045–1050, Jun. 2017.
[9] K. Sarabandi and N. Behdad, "A frequency selective surface with miniaturized elements," *IEEE Trans. Antennas Propag.*, vol. 55, no. 5, pp. 1239–1245, May 2007.
[10] T. K. Wu, *Frequency Selective Surface and Grid Array*. New York, NY, USA: Wiley, 1995.
[11] H. Li, C. Yang, Q. Cao, and Y. Wang, "An ultrathin bandpass frequency selective surface with miniaturized element," *IEEE Antennas Wireless Propag. Lett.*, vol. 16, pp. 341–344, 2017.
[12] A. B. Varuna, S. Ghosh, and K. V. Srivastava, "An ultra thin polarization insensitive and angularly stable miniaturized frequency selective surface," *Microw. Opt. Technol. Lett.*, vol. 58, no. 11, pp. 2713–2717, Nov. 2016.
[13] T. Hong, M. Wang, K. Peng, and S. Gong, "Ultrathin and miniaturized frequency selective surface with closely located dual resonance," *IEEE Antennas Wireless Propag. Lett.*, vol. 18, no. 6, pp. 1288–1292, Jun. 2019.
[14] G. Itami, Y. Toriumi, and Y. Akiyama, "A novel design method for miniaturizing FSS based on theory of meta-materials," in *Proc. Int. Symp. Antennas Propag. (ISAP)*, Oct. 2017, pp. 1–2.
[15] F. Bilotti, A. Toscano, K. B. Alici, E. Ozbay, and L. Vegni, "Design of miniaturized narrowband absorbers based on resonant-magnetic inclusions," *IEEE Trans. Electromagn. Compat.*, vol. 53, no. 1, pp. 63–72, Feb. 2011.
[16] E. A. Parker and A. N. A. El Sheikh, "Convoluted array elements and reduced size unit cells for frequency-selective surfaces," *IEE Proc. H-Microw., Antennas Propag.*, vol. 138, no. 1, pp. 19–22, Feb. 1991.
[17] A. A. Dewani, S. G. O'Keefe, D. V. Thiel, and A. Galehdar, "Window RF shielding film using printed FSS," *IEEE Trans. Antennas Propag.*, vol. 66, no. 2, pp. 790–796, Feb. 2018.
[18] G. Catton, H. G. Espinosa, A. Dewani, and S. G. O'Keefe, "Simulation of S- and L-band FSS reflector antenna," in *Proc. Austral. Microw. Symp. (AMS)*, Feb. 2018, pp. 69–70.
[19] S. J. Orfanidis, "Linear and loop antennas," in *Electromagnetic Waves and Antennas*, vol. 4. Piscataway, NJ, USA: Rutgers Univ. Press, 2016, ch. 17, sec. 17, p. 783. [Online]. Available: http://eceweb1.rutgers.edu/~orfanidi/ewa/
[20] S. A. P. Rizvi and R. A. A. Khan, "Klopfenstein tapered 2-1 GHz microstrip Balun," in *Proc. IEEE Appl. Sci. Technol. (IBCAST)*, Islamabad, Pakistan, Jan. 2012, pp. 165–168.
[21] Telstra, Melbourne, VIC, Australia. (2014). *Finding the Right Spot*. Accessed: Jan. 20, 2021. [Online]. Available: https://www.telstra.com.au/content/dam/tcom/personal/broadband/pdf/nbn-finding-the-right-spot-fixed-wireless.pdf

GARTH D. CATTON (Member, IEEE) received the B.Eng. degree (Hons.) in electronics and computers from Griffith University, Brisbane, QLD, Australia, in 2016, where he is currently pursuing the Ph.D. degree in electrical engineering.

He was a Control Systems Research Intern with the Sirindhorn International Institute of Technology (SIIT), Thammasat University, Bangkadi, Pathum Thani, Thailand. His current research interests include the development of high-gain antennas using FSS and Fabry–Perot cavity antennas.

HUGO G. ESPINOSA (Senior Member, IEEE) received the bachelor's degree in electronics and telecommunications engineering from the Monterrey Institute of Technology and Higher Education, Mexico, in 1998, the master's degree in electrical engineering from the University of São Paulo, São Paulo, Brazil, in 2002, and the Ph.D. degree *(summa cum laude)* in electrical engineering from the Technical University of Catalonia, Barcelona, Spain, in 2008.

He has been a Visiting Researcher with the Federal Polytechnic School of Lausanne, Lausanne, Switzerland. He is currently a Postdoctoral Fellow with the School of Electrical Engineering, Tel Aviv University, Tel Aviv, Israel. Since 2011, he has been with the School of Engineering and Built Environment, Griffith University, Brisbane, QLD, Australia, where he is currently a Lecturer in electronic engineering. His research interests include computational electromagnetics, antennas and propagation, wireless sensor networks, inertial sensors, and wearable sensor technology for human monitoring.

ALIYA A. DEWANI (Member, IEEE) received the B.Eng. degree (Hons.) from the University of Kashmir, Srinagar, India, in 2005, the M.Eng. degree from University Technology Malaysia, Malaysia, in 2007, and the Ph.D. degree in electrical engineering from Griffith University, Brisbane, QLD, Australia, in 2016.

Her doctoral research focused on the analysis and design of frequency-selective surfaces on thin conformal transparent substrates using screen printing technology. Her current research interests include computational electromagnetics, design and modeling of engineered structures with novel electromagnetic behaviour, multiple scattering, and antenna measurements.

STEVEN G. O'KEEFE received the B.Sc. degree in physics, mathematics, and electronics from Griffith University, Brisbane, QLD, Australia, in 1985, the B.Sc. degree (Hons.) in electronics and the M.Sc. degree in biomedical electronics from La Trobe University, Melbourne, VIC, Australia, in 1986 and 1990, respectively, and the Ph.D. degree in geophysical electromagnetics from Griffith University, in 1996.

He is currently an Associate Professor and the Head of electronic engineering with the Griffith School of Engineering and Built Environment, Griffith University. His current research interests include compact mobile antenna design and electromagnetic geophysics.